J. COMBIN. MATH. COMBIN. COMPUT. 127a (2025) 8527--8545

Journal of Combinatorial Mathematics and Combinatorial Computing
www.combinatorialpress.com/jcmcc

Simulation of Shallow Natural Gas Distribution in Tunnel Construction Area and Calculation of Elasticity Parameters Based on Pre-stacked AVO Inversion Technology

Bochuan Geng[1,✉], Peidong Su[1], Xinhua Tao[2], Xiangang Zhu[2], Jiang Yu[2]

[1] College of Geosciences and Technology, Southwest Petroleum University, Chengdu, Sichuan, 610500, China
[2] China Railway Communications Investment Group Co., LTD, Nanning, Guangxi, 530219, China

ABSTRACT

Tunnel gas and shallow natural gas overflow have been a major problem plaguing the safe construction of tunnels and one of the main types of common diseases in tunnel engineering. The article chooses the tunnel construction of Funci Highway as the research object, and collects the rock and gas data in the research area on the basis of analyzing the distribution characteristics of shallow natural gas. Based on the AVO analysis technique, the PP wave reflection coefficient is approximated as a linear combination of longitudinal wave velocity, transverse wave velocity, density and other elastic constants to construct a pre-stack AVO inversion model to analyze the shallow natural gas distribution in the Funci Highway Tunnel construction. The porosity of the rock layer in the tunnel construction area ranges from 4.5% to 12%, with an average porosity of 8.93% and a maximum permeability of 0.004 μm^2. The longitudinal wave impedance distribution of the non-reservoir surrounding rock ranges from 1.48 to 2.01, and the error between the longitudinal wave velocity and density obtained by the inversion and the original logging curves is up to only 2.04%. Combined with the logging data, it can realize the comprehensive evaluation of the oil and gas geological environment of Funci Highway tunnel construction, and provide data support for ensuring the safety of Funci Highway tunnel construction.

Keywords: longitudinal wave velocity; AVO technology; inversion model; porosity; shallow natural gas; Funci Expressway

1. Introduction

In the preparation stage of tunnel construction, some managers often do not do their job in controlling

✉ Corresponding author.
E-mail address: gbchuan@126.com (B. Geng).
Received 03 March 2024; Revised 20 April 2024; Accepted 10 November 2024; Published Online 15 April 2025.
DOI: 10.61091/jcmcc127a-471

the safety risks of tunnel projects. The risk control as well as management of tunnel engineering construction is not in place, leading to the occurrence of safety accidents [1-4]. With the rapid development of infrastructure, the construction of highway tunnels has been accelerated, creating favorable conditions for driving economic development [5-6]. However, due to the relatively large number of hidden dangers in tunnel construction, if not managed effectively, it will cause safety and quality problems, affecting the reliability of the project, which will lead to serious consequences [7-9]. Tunnel construction is a high-risk engineering activity, involving personnel safety, equipment safety, environmental protection and other aspects, so in tunnel construction, safety management should be strengthened, and management requirements should be strictly enforced in accordance with the characteristics of the project, and risk warning technology should be reasonably applied to prevent accidents from occurring [10-13].

As a kind of unconventional natural gas, shallow natural gas is located in geological conditions and its own characteristics are different from deep natural gas, with wide distribution, shallow burial, thin gas layer, low pressure, gas and water in the same layer, loose reservoir and large changes, etc., the cost of using conventional oil and gas exploration methods is high and the economic benefits are low [14-17]. Therefore, its exploration method is different from that of deep natural gas, and the existing simple, cheap and effective exploration means should be selected in order to achieve the purpose of breakthrough in a short period of time [18-19].

Tunneling operations in shallow natural gas-containing soils may cause tunnel displacement, fracture, or pit instability due to the release of shallow natural gas, resulting in irreparable and significant economic losses. The article selects the tunnel construction area of Hunan Furnace Hongshan-Cili Expressway as the research object, analyzes the geological background and regional tectonic situation of the area, and describes the distribution characteristics of shallow natural gas and the hazards of tunnel construction. The gas logging data and rock slice identification are used to obtain rock and gas samples, and the pre-stack AVO inversion model is constructed based on AVO technology and linear combination of elastic constant terms. Based on the logging data, the reservoir characteristics of the tunnel construction area of Funci Highway are analyzed, and the pre-stack AVO inversion model is used to analyze the shallow natural gas distribution in the tunnel construction area of Funci Highway and carry out a comprehensive evaluation of the tunnel oil and gas, aiming to improve the safety of the tunnel construction of Funci Highway.

2. Selection of study area and shallow natural gas exploration

In order to drive and accelerate the development of regional economic construction between Furnace Hongshan and Cili County in Hunan Province, the construction of the highway helps to realize the rapid connection between the two areas. Due to the relatively shallow depth of the highway tunnel, the hydrocarbon source rock in the area is relatively old, and does not have the possibility of generating natural gas after Yanshan, Himalayan and recent tectonics. However, under the action of ancient geological structures, the deep natural gas migrates upward along the joints and fissures or fractures to dip the tunnel through the strata and form secondary natural gas reservoirs in the strata. During the construction of these tunnels, there is a possibility of encountering shallow natural gas, which may lead to combustion and explosion, jeopardizing the construction safety, so it is particularly important to carry out comprehensive detection of shallow oil and gas in the Fenzhi Expressway Tunnel.

2.1. Geological background of the study area

2.1.1. Location of work areas. Hunan furnace red mountain to Cili highway, the route from Changde City, Shimen County and Yichang City, Wufeng Tujia Autonomous County, the junction of the furnace red mountain (Hunan-Egypt border), connected to the construction of the Huobei high-speed Yidu (Quanfu River) to the Hubei-Xiangjiang boundary section. By Taiping, Baizhang hillock, Weixin, Guotaiqiao, Dongyueguan, Linjiadai, stopping at Cili County West Zhangjiazhan, connected to the built Hohoku Expressway Cili to Zhangjiajie section, a total length of about 80 kilometers. Figure 1 for the stove red mountain to Cili highway road map. The route of Sanglong Expressway Project starts from Hongjiaguan Township of Sangzhi County to connect with the constructed Zhangjiajie-Sangzhi Expressway, passes through Chenjiahe Township and Shanghexi Township, and then enters into the territory of Longshan County, passes through Shuitianba Township and Tsiyantang Township, and stops at Maoping Township to connect with the constructed Longshan-Yongshun Expressway, with a length of about 61.45 kilometers.

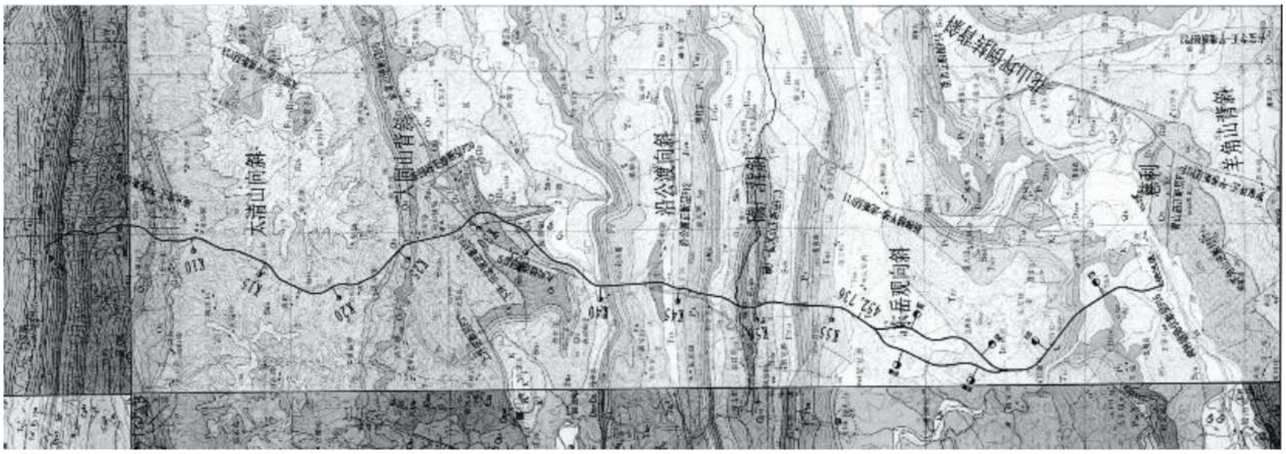

Fig. 1. The red mountain to the CiLi highway road map

The region has developed gullies and a large number of streams, which have obvious seasonal river characteristics due to the influence of topography and climate. That is, the flow is small or dry in the dry season, flooding in the flood season, and the river flow varies greatly during the year. Rainy season mountain surface water into the gully and through the gully drainage, gully water flow can be up to 5 to 10 times the usual flow, dry season stream flow is small, or even cut off, for the typical mountain type stream. Highway design should take safety protection measures to prevent the roadbed and bridge abutment from flood hazards.

2.1.2. Regional tectonics:

1) Tectonic evolution. Northwest Hunan is located in the northwestern region of Hunan Province, belonging to the Yangzi Plateau area, and the study area from the Aurignacian to the Early Paleozoic is a passive continental margin on the southeastern edge of the Upper Yangzi landmass. At the end of the Caledonian, the collision between the Huaxia Plate and the Yangzi Plate produced a westward retrograde thrusting effect, and a marginal fold belt consisting of large retrograde fractures and folds appeared in the western part of Northwest Hunan Province, forming a complex tectonic condition dominated by the two major tectonic systems of the north-east tectonic system and the north-east tectonic system. The arrangement of ruptures and folds in the area is characterized by the distribution of groups, with certain genesis links and similar combinations.

2) Tectonic features. Hunan Province is located in the southern part of the second complex subsidence belt of the Neohuaxian system and the second complex uplift belt of the Neohuaxian system in the East Asian continent, and north of the middle part of the latitudinal tectonic belt of the South Ridge. Generally speaking, Hunan Province has developed many tectonic systems, including east-west tectonic system, north-south tectonic system, various torsional tectonic systems, north-west tectonic system, and other tectonic systems with unknown system affiliation. The outline of its distribution is that Hunan belongs to the northern part of the middle section of the Nanling giant latitudinal tectonic

belt, and there are three regional east-west tectonic belts crossing the province in central and northern Hunan. Bounded by the Shimen-Anhua-Wugang line, the east and west sides are respectively the second subsidence zone and the second uplift zone of the Neo-Chinese tectonic system, with the Huaxia tectonic system hidden in between. In the south and center, there is a north-south tectonic belt and a mountain-type tectonic structure with the top of the arc facing west. At the same time, there are various types of spiral tectonics in the center. In terms of tectonic patterns, the province can be roughly divided into two areas with obvious differences. Northwestern Hunan is dominated by wide, gently spreading folds, with ruptures taking second place. In central and southern Hunan, there are mostly box-shaped compact folds, and the fracture structure is extremely developed.

Figure 2 shows the geotectonic map of the study area. Cili County is located in the northwest of Hunan, an arc-shaped tectonic belt protruding to the north and west of the arc of the turning part, crustal tectonics is more complex, according to the tectonic system of the spread and interrelationships, can be divided into the following four categories:

1) Huaxia system tectonics, spread in the southwest of the county. From north to south, there are DuTanPing - NanshanPing fracture, WubaoXi backward sloping, ChenJiaWan oblique, south public collapse into the scissors temple fracture, FeiYanYa backward sloping, hole creek - gold collapse fracture and the silk Mao collapsed oblique.

2) Regional east-west tectonics, spread in the northern part of the county. From the south to the north, there are mainly the open Sanguansi Temple dyke and the tight Zhuangzhuang collapse dyke, the Longtanwan dyke and the Xiangjiaxi dyke, and so on.

3) The new Huaxia system, which can only be seen in the western edge of the county, is the north-north-east oriented Yujiazui to Sanguansi dyke.

4) Turbulent torsional tectonics, spreading in the eastern part of the county, consists of a number of pressure-torsional fractures and axially curved folds with curved arcs and steep inclination angles.

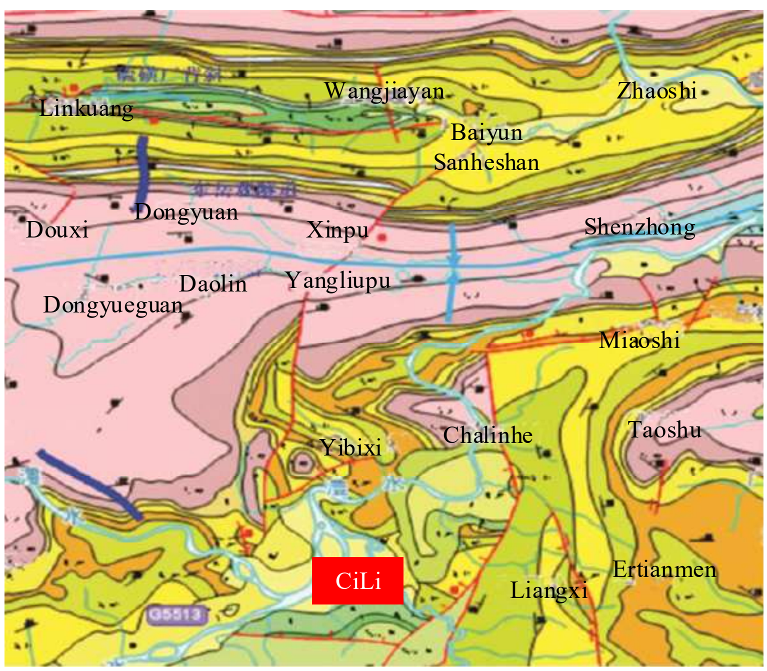

Fig. 2. Geological map of the research area

The hydrocarbon source rocks in the area are relatively old, and after Yanshan, Himalayan and recent tectonic modification, the gas reservoirs have been damaged more seriously, and it is probable that large-scale gas reservoirs cannot be formed, but the formation of small-scale natural gas aggregation due to suitable closure conditions cannot be excluded. Combined with the regional geological data and field investigation, most of the hydrocarbon rock layers in the area are directly exposed on the surface, with the possibility of lateral dispersion, which affects the preservation of natural gas. However, there are more reverse faults developed in the area, and most of the faults are open faults, which provide a passageway for the transportation of shallow natural gas, and can play a certain positive role in the preservation conditions. The shallow natural gas risk level of the tunnel project needs to be further determined by analytical tests in the field and indoor.

2.2. Shallow natural gas distribution characteristics and hazards

2.2.1. Characteristics of shallow natural gas distribution. According to the existing railroad tunnel technical specifications on the classification methods and standards for gas tunnels, low-gas work areas and high-gas work areas can be determined by the absolute gas outflow, when the gas outflow of the whole work area is less than $0.5m^3/min$, it is a low-gas work area, and when it is greater than or equal to $0.5m^3/min$, it is a high-gas work area. From the point of view of the existing normative division standards and methods, this is a big difference with shallow natural gas, mainly in:

1) Shallow natural gas is not the deep industrial and civil gas reservoirs sought by the petroleum and geological drilling department, and its pressure and concentration are very low, which cannot be measured under normal circumstances.

2) The depth of railroad gas tunnels is generally shallow, and the natural gas obtained by geological drilling is non-industrial and civil gas, with weak pressure and little gas volume, which makes measurement and calculation quite difficult.

3) The tunnel body passes through the section is generally non-hydrocarbon geological rock layer, the shallow natural gas in the tunnel is the underground oil and gas along the geological tectonic movement formed in the tectonic fissure, fault fracture zone voids and other channels, from deep to shallow, from the bottom to the top, with the long geologic era of change, transportation, and gradually upward to the shallow strata of the ground immersion in the formation of the large tectonic fissures, fault fracture zones, the large void formed in the independent gas capsule body. The formation pattern of gas pockets is shown in Figure 3, and its reserves and distribution are characterized by large differences, random changes and uncertainties. Therefore, tunnel natural gas prediction and forecasting also have randomness and uncertainty.

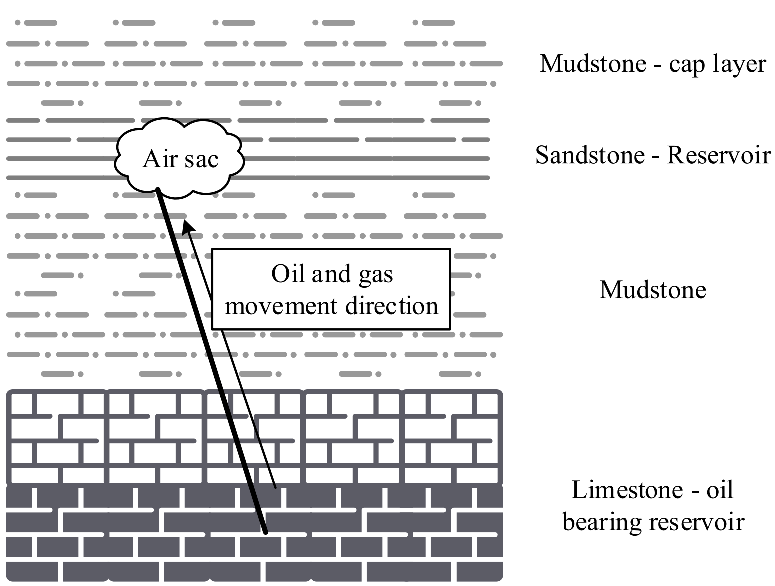

Fig. 3. Tunnel balloon formation pattern

In summary, the degree of development of shallow natural gas is closely related to the geological paleotectonic background (subduction tectonics) in which it is located and the shallow geological formations.

2.2.2. Natural gas hazards to tunnel construction. A gas field has been discovered in the vicinity of the high speed tunnel construction, and based on the tectonic features there may be significant gas-bearing formations, as well as land-phase shallow oil and gas assemblages. The main construction risks are as follows:

1) As natural gas is rich in methane, hydrogen sulfide and other flammable components, it will burn or even explode when it reaches a certain concentration, which will seriously jeopardize the safety of human beings and equipment.

2) Hydrogen sulfide and other toxic gases, inhalation will cause personal injury.

3) Hydrogen sulfide is also highly corrosive, causing harm to people and equipment, and affecting the work schedule.

When the high-speed tunnel passes through the gas field area or closed tectonic ring, it may encounter natural gas. Therefore, it is one of the work contents of this tunnel special geological investigation study to assess the natural gas hazard of the tunnel in this area, to provide a basis for the design and construction, and to take corresponding engineering measures to ensure the safety of construction and operation.

3. Natural gas inversion model based on AVO technology

AVO technology is a technology to study the change of seismic reflection wave amplitude with the gun check distance, analyze the change rule in the pre-stacked channel set, get the elastic parameters of the rock, discriminate the lithology and pore filling, in order to achieve the purpose of directly searching for natural gas reservoirs. In the process of high-speed tunnel construction, it is clear that the shallow natural gas situation in the construction area can help the excavation of the tunnel in the later stage, and through the support of real and reliable data to avoid the risk area of high-speed tunnel construction in advance, so as to ensure the safety of high-speed tunnel construction.

3.1. Data Acquisition and Characterization of Thin Slices

3.1.1. Field Gas Logging. Gas logging is the most direct means of determining the gas content of underground cores. During the drilling process, if the drilling encounters a hydrocarbon layer, the oil and natural gas will enter the drilling fluid through filtration and diffusion. Gas logging is a logging method that directly measures the content and composition of natural gas in the drilling fluid to determine the nature of oil and gas in the drilled formation, and this method can detect oil and gas shows in time.

The main gas logging equipments used in this gas testing project of Fuzi Highway Tunnel are SK3Q01 hydrogen flame chromatograph, YH Technology 615L industrial control computer, SK-7T06 explosion-proof electric degasser, SK3Q01 hydrogen flame chromatograph can complete the analysis of $C_1 \sim C_5$ and blowback in 5 minutes, and complete the analysis of $C_1 \sim C_4$ and blowback in 2 minutes, and the separability of C_1/C_2 is good. It can accurately measure the group stratum, tectonics, natural gas concentration and other information to comprehensively determine the gas category of the tunnel for tunnel construction design services.

1) Sampling standard. In the middle of each tunnel borehole, near the bottom plate to take rock samples of each group, drilling encounter coal seams, carbonaceous mudstone, etc., according to the actual situation of the appropriate encryption, rock samples require a length of 10-20cm, on-site encapsulation.

2) Gas collection. In order to quantitatively analyze the main components of the gas in the tunnel stratum, the gas near the tunnel palm face was collected. The gas collection method is mainly the

gunnel method, by drilling a gunnel into the palm face and sealing it at the base of the gunnel. Then the gas collection hose was passed through the borehole to the rock body, and finally the gas collection was carried out through the suction ball.

3.1.2. Identification of rock fragments. Thin section identification is a method of identifying transparent minerals and rocks under a polarized light microscope. Mineral or rock specimens ground into thin slices, under the polarized light microscope to observe the crystallization characteristics of minerals, determine its optical properties, determine the mineral composition of the rock, study its structure, structure, analyze the order of mineral generation, determine the type of rock and its genesis characteristics, and finally set out the name of the rock.

Thin section identification method is an important method often used in geological mineral searching work, also applied to other industries, agriculture and medicine. Polarized light microscope is used to study the so-called transparent and opaque anisotropic materials of a kind of microscope, the principle is that all have birefringent material, in the polarized light microscope will be able to distinguish clearly. Reflective polarizing microscope is a necessary instrument to study and identify the birefringent materials by using the polarization property of light, which can be used for single polarized light observation, orthogonal polarized light observation and cone light observation. With reference to the requirements of rock flake identification, this flake identification mainly adopts Leica type polarizing microscope. This polarizing microscope has the advantages of integrating camera and software module, easy operation and so on.

3.2. Pre-stack AVO inversion modeling

3.2.1. Basic Theory of AVO Analysis. AVO technology is based on the theory of elastic waves, through the in-depth study of the dynamic properties under the action of seismic waves and the relationship between formation lithology [20]. By using AVO forward simulation, the AVO characteristics of oil, gas, water and lithology can be known, which provides a basis for the qualitative prediction of oil and gas reservoirs, and the change of amplitude with the angle of incidence itself contains important information about the lithological and tectonic coefficients. The AVO relationship can be used to directly invert the physical parameters of the rock mass, and then use these parameters to characterize the reservoir structure qualitatively or quantitatively.

Assume that there are two layers of media with different elastic parameters above and below the interface. The elastic parameters above the interface are V_{p1}, V_{zl} and ρ_1, and the elastic parameters below the interface are V_{p2}, V_{z2} and ρ_2. Based on Huygens' principle, when a P-wave propagates to a reflection point at an interface, that point can be considered as a new source and continues to propagate in the upper and lower media. Seismic waves in the incident and transmitted media are called incident and transmitted waves, respectively. Their intrinsic relationship should satisfy Snell's law, viz:

$$\frac{\sin\alpha}{V_{p1}} | = \frac{\sin\beta}{V_{s1}} = \frac{\sin\alpha'}{V_{p2}} = \frac{\sin\beta'}{V_{s2}} = P \tag{1}$$

where α and β represent the reflection angles of the reflected longitudinal wave and the reflected converted wave, respectively. α' and β' represent the transmission angle of the transmitted longitudinal wave and the transmitted converted wave, respectively. The relationship between the angles and velocities of incident, reflected and transmitted waves can be reflected by the formula.

Based on the theory of seismic wave dynamics, the relationship between the reflection and transmission coefficients of P- and S-waves can be expressed using the Zoplitz equation, i.e.:

$$\begin{bmatrix} \sin\alpha & \cos\beta & -\sin\alpha' & \cos\beta' \\ \cos\alpha & -\sin\beta & \cos\alpha' & \sin\beta' \\ \sin 2\alpha & \frac{V_{p1}}{V_{z1}}\cos 2\beta & \frac{V_{p1}}{V_{p2}}\frac{V_{z2}^2}{V_{z1}^2}\frac{\rho_2}{\rho_1}\sin 2\alpha' & -\frac{V_{p1}}{V_{z2}}\frac{\rho_2}{\rho_1}\sin 2\beta' \\ -\cos 2\beta & \frac{V_{z1}}{V_{p1}}\sin 2\beta & \frac{V_{p2}}{V_{p1}}\frac{\rho_2}{\rho_1}\cos 2\beta' & \frac{V_{z2}}{V_{p1}}\frac{\rho_2}{\rho_1}\sin 2\beta' \end{bmatrix} \begin{bmatrix} R_{pP} \\ R_{pP} \\ T_{pP} \\ T_{pS} \end{bmatrix} = \begin{bmatrix} -\sin\alpha \\ \cos\alpha \\ \sin 2\alpha \\ \cos 2\beta \end{bmatrix} \quad (2)$$

where R_{pp} and R_{ps} are the reflection coefficients of the reflected P-wave and reflected SV-wave, and T_{pp} and T_{ps} are the transmission coefficients of the transmitted P-wave and transmitted SV-wave, in that order [21].

3.2.2. Pre-stack AVO inversion methods. Under the assumption of small variations of elastic parameters on both sides of the interface, the PP wave reflection coefficient is approximated as a linear combination of three elastic constant terms in terms of longitudinal wave velocity, transverse wave velocity, and density, viz:

$$R_{pp}(\theta) = \left(\frac{1}{2}+\frac{1}{2}\tan^2\theta\right)\frac{\Delta V_p}{V_p} + \left(\frac{-4\sin^2\theta}{\gamma_{sat}^2}\right)\frac{\Delta V_s}{V_s} + \left(\frac{1}{2}-\frac{2\sin^2\theta}{\gamma_{sat}^2}\right)\frac{\Delta\rho}{\rho} \quad (3)$$

where, ΔV_P is the difference between the upper and lower longitudinal wave velocities at the interface, ΔV_S is the difference between the upper and lower transverse wave velocities at the interface, $\Delta\rho$ is the difference between the upper and lower densities at the interface, V_P is the mean value of the upper and lower longitudinal wave velocities, V_S is the mean value of the upper and lower transverse wave velocities, ρ is the mean value of the upper and lower densities, θ is the angle of incidence, and $\gamma_{za} = (VpVS)za$ is the team transverse wave velocity ratio of the saturated rock [22].

It is assumed that the longitudinal wave velocity V_P and transverse wave velocity V_S of the rock in the above equation are frequency dependent, and it is assumed that the density does not vary with frequency. Therefore, the frequency dependence of V_P and V_S leads to the variation of the reflection coefficient with frequency ω. Therefore, by extending the AVO approximation in the above equation with respect to longitudinal and transverse wave velocities to the frequency-dependent form, the frequency-dependent reflection coefficient equation is established as:

$$R_{pp}(\theta) = \left(\frac{1}{2}+\frac{1}{2}\tan^2\theta\right)\frac{\Delta V_p}{V_p}(\omega) + \left(\frac{-4\sin^2\theta}{\gamma_{sat}^2}\right)\frac{\Delta V_s}{V_s}(\omega) + \left(\frac{1}{2}-\frac{2\sin^2\theta}{\gamma_{sat}^2}\right)\frac{\Delta\rho}{\rho} \quad (4)$$

Let the coefficients be respectively:

$$\begin{cases} A(\theta) = \frac{1}{2}+\frac{1}{2}\tan^2\theta \\ B(\theta) = \frac{-4\sin^2\theta}{\gamma_{sat}^2} \\ C(\theta) = \frac{1}{2}-\frac{2\sin^2\theta}{\gamma_{sat}^2} \end{cases} \quad (5)$$

Eq. (4) is simplified and expressed as:

$$R_{pp}(\theta) = A(\theta)\frac{\Delta V_p}{V_p}(\omega) + B(\theta)\frac{\Delta V_s}{V_s}(\omega) + C(\theta)\frac{\Delta\rho}{\rho} \tag{6}$$

Define D_P and D_S as the dispersion properties associated with the longitudinal wave velocity V_P and transverse wave velocity V_S, then:

$$\begin{aligned} D_p &= \frac{\partial}{\partial\omega}\left(\frac{\Delta V_p}{V_p}\right) \\ D_s &= \frac{\partial}{\partial\omega}\left(\frac{\Delta V_s}{V_s}\right) \end{aligned} \tag{7}$$

The dispersion property in Eq. (7) is estimated using the following frequency-varying AVO inversion formula.

First, Eqs. (6) and (7) are organized as:

$$\Delta R_{pp} = R_{pp}(\theta,\omega) - R_{pp}(\theta,\omega_0) = (\omega-\omega_0)\left[A(\theta)D_{Mc} + B(\theta)D_\mu\right] \tag{8}$$

Considering the seismic subwave effects, both sides of Eq. (8) are obtained by multiplying the subwave spectrum $W(\omega)$:

$$\Delta S = S(\theta,\omega) - S(\theta,\omega_0) = (\omega-\omega_0)W(\omega)\left[A(\theta)D_{\Lambda k} + B(\theta)D_\mu\right] \tag{9}$$

where ΔS is the time-frequency spectrum corresponding to the AVO data computed by the time-frequency method and $W(\omega)$ can be estimated from the data.

After that, the matrix form corresponding to Eq. (9) is given to realize the frequency-varying AVO inversion, i.e:

$$\begin{bmatrix} \Delta S(\theta_1,\omega_1) \\ \vdots \\ \Delta S(\theta_1,\omega_m) \\ \vdots \\ \Delta S(\theta_n,\omega_1) \\ \vdots \\ \Delta S(\theta_n,\omega_m) \end{bmatrix} = \begin{bmatrix} W(\omega_1)(\omega_1-\omega_0)A(\theta_1) & W(\omega_1)(\omega_1-\omega)B(\theta_1) \\ \vdots & \vdots \\ W(\omega_m)(\omega_m-\omega_0)A(\theta_1) & W(\omega_m)(\omega_m-\omega_0)B(\theta_1) \\ \vdots & \vdots \\ W(\omega_1)(\omega_1-\omega_0)A(\theta_n) & W(\omega_1)(\omega_1-\omega_0)B(\theta_n) \\ \vdots & \vdots \\ W(\omega_m)(\omega_m-\omega_0)A(\theta_n) & W(\omega_m)(\omega_m-\omega_0)B(\theta_n) \end{bmatrix} \begin{bmatrix} D_{Ak} \\ D_\mu \end{bmatrix} \tag{10}$$

In this case, the time-frequency analysis of the AVO data for n incidence angle is decomposed into m frequency components to obtain the spectrum $\Delta S(\theta,\omega)$.

Eq. (9) can be expressed by the matrix as:

$$S = C\begin{bmatrix} D_{Mc} \\ D_\mu \end{bmatrix} \tag{11}$$

where s is the spectrum $\Delta S(\theta,\omega)$, C is the coefficient matrix.

The dispersion property is inverted using the least squares method, i.e:

$$\begin{bmatrix} D_{Mc} \\ D_\mu \end{bmatrix} = \left(C^T C + \sigma^2 I\right)^{-1} C^T S \tag{12}$$

where σ is the damping factor and I denotes the unit matrix.

3.2.3. Pre-stack AVO inversion process. Previous researchers have studied and analyzed the characteristics of shallow natural free gas using post-stack and pre-stack inversion. This paper focuses on the hydrate layer, hydrate and free gas coexistence layer, and local free gas layer in the target area, and utilizes the pre-stack simultaneous inversion to study the distribution of the hydrate layer and free gas layer, so as to provide support for the comprehensive evaluation of oil and gas in the process of high-speed tunnel construction.

The technical process centered on the pre-stack simultaneous inversion is shown in Fig. 4. Based on the AVO feature inversion of the pre-stack data, the elastic parameters such as longitudinal wave velocity, transverse wave velocity, density, longitudinal impedance, longitudinal and transversal wave velocity ratio, Poisson's ratio, etc. are obtained, and the sensitivity parameter is selected to reveal the differences between the hydrate layer, hydrate-free gas coexisting layer, and free gas layer, so as to get the spatial distributions of the hydrate and the free gas finally.

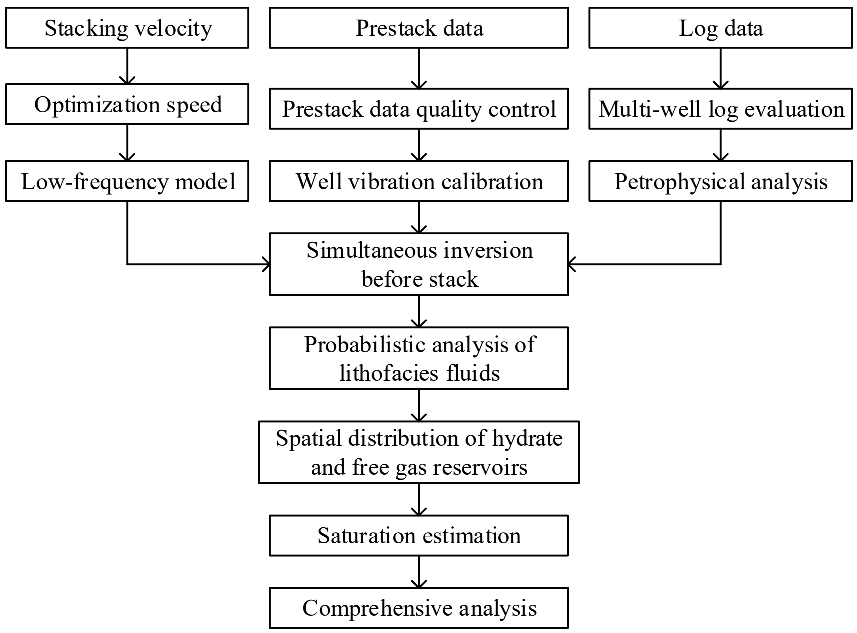

Fig. 4. Prestack Inversion workflow

4. Fuzi Expressway Tunnel Construction Safety and Oil and Gas Evaluation

The number of cases of encountering shallow gas strata during high-speed tunnel construction is gradually increasing, which brings many safety hazards to high-speed project construction. Due to the irregular distribution of the underground gas layer, the gas pressure of the chambers is different, and the bearing capacity of each chamber for the overlying soil layer is also very different, which results in too large a difference in the ground settlement after the release of the shallow gas, and then irreversible deformation and damage of the tunnel structure occurs. This chapter is based on the high speed tunnel construction project from Fuhongshan to Cili County in Hunan Province as an example, and adopts AVO technology to analyze the oil and gas in the tunnel construction of Fuci High Speed Tunnel, in order to provide support for ensuring the safety of Fuci High Speed Tunnel construction.

4.1. Regional reservoir characterization

4.1.1. Porosity and permeability. Based on the formation data in the area from Furnace Hongshan to Cili County, it is known that the lithology of the reservoirs of Longmaxi Formation, Qixia Formation and Wujiaping Formation is mudstone and carbonate rock. The reservoirs are mainly intergranular solution holes, dissolution enlarged holes, followed by intragranular solution holes, cast holes and residual intergranular holes, and cracks are occasionally seen. The core porosity and permeability were calculated, and the distribution histograms of core porosity and permeability in the region were obtained as shown in Fig. 5, and the porosity-permeability correlation was shown in Fig. 6. Among them, Fig. 5(a) and (b) show the distribution histograms of porosity and permeability, respectively.

The porosity of the formations in the region is distributed between 4.5% and 12%, mainly in the interval of 6% to 10%, with an average porosity of 8.93%. The maximum permeability is 0.004μm^2, mainly distributed between 0.001~0.004μm^2. The rock structure in the area of Funci Highway Tunnel Project exposes a small amount of strata in the axial part, and the Cretaceous strata are exposed at the surface of the two flanks. Therefore, in the two flanks of the tectonic structure, the capping conditions of the reservoirs are good, the capping conditions of the reservoirs in the middle and upper part of the tectonic axis are relatively poor, and the capping conditions of the reservoirs in the middle and lower part of the tectonic axis are relatively good. Under the analysis of the porosity of the rock layer, it can be understood that the fault closure effect becomes weaker with the decrease of the burial depth of the fault, so the upper fault in the region plays a destructive role in the gas reservoir. However, if the sand body is not in direct contact with the fault, it can still rely on the lateral confinement of the mudstone to prevent the oil and gas from being dispersed longitudinally along the section. Therefore, when carrying out high-speed tunnel construction, attention must be paid to the local shallow natural gas enrichment in the area of faults and joint fissures.

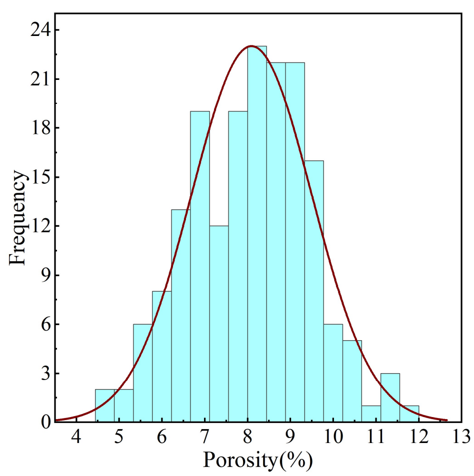

(a) Porosity

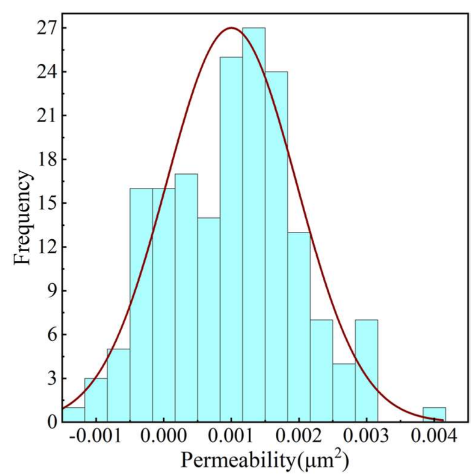

(b) Permeability

Fig. 5. Distribution histogram of porosity and permeability

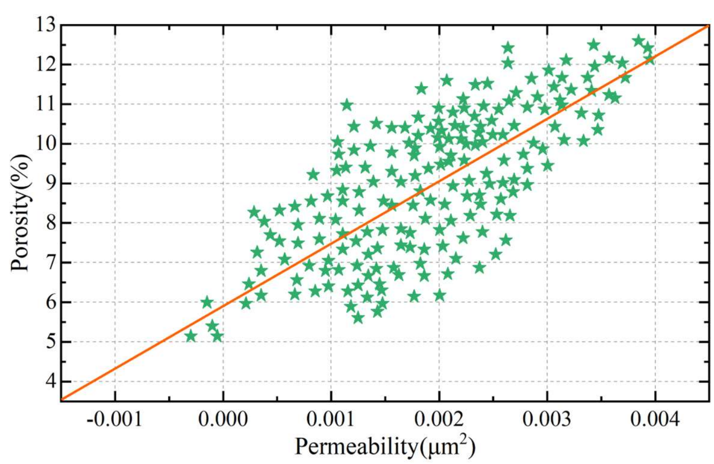

Fig. 6. Porosity - correlation of permeability

4.1.2. Crack development. In order to further understand the fracture development of the rock formations in the tunnel construction area of Furnace Ci Highway, the sandstones of Longmaxi Formation, Qixia Formation, and Wujiaping Formation were analyzed for porosity-permeability relationships. Figure 7 shows the results of the fracture development condition, in which Figures 7(a) and (b) show the porosity-permeability relationships of sandstones from different regions and different sections of the gas reservoir.

In general, the sandstone in the construction area of Funci Highway Tunnel has a good porosity-permeability relationship, and the analysis of the pre-pressure pressure recovery data of the gas reservoir wells also shows the characteristics of a single-medium, pore-type reservoir. However, cracks can be seen in some samples. According to the statistics of physical properties of sandstone in the construction area of Funci Highway Tunnel, 25% of the samples with porosity greater than 6% have permeability less than 0.002μm^2, and 20% of the samples with porosity greater than 10% have permeability less than 0.004μm^2. Therefore, fracture development can improve the reservoir percolation capacity to a certain extent, so that some sandstones with porosity reaching the standard of high-quality reservoirs can have the permeability corresponding to high-quality reservoirs at the same time.

The sandstone at the bottom of L1 section has significantly lower porosity than the sandstone in L2~L3 sections. However, when the porosity is greater than 8%, corresponding to the same porosity, the sandstone in the L1 section has a larger median radius and higher permeability, indicating that there are a large number of microfine seams in the sandstone. These microfine intragranular and marginal seams are short in extension, widely distributed, and similar in size to matrix pore throats, so they can be attributed to the matrix pore system. Microfine seams usually occur in sandstones with high quartz, high feldspar, and low clasts. Meanwhile, microseams are relatively more developed in L3 gas reservoirs in areas where faults are developed, such as the main body and the southeast flank of the Longmaxi and Qixia Formations. The permeability of sandstones in the Wujiaping Formation is generally greater than 0.01 μm^2, of which the II and III reservoirs account for 40%~65%, and the I reservoirs only account for 10%. According to statistics, permeability <0.01μm^2 in samples with porosity >8% accounts for 25%~40%, and permeability <0.1μm^2 accounts for 55%~60%. Therefore, the fracture is crucial to the improvement of reservoir percolation capacity, and the degree of fracture development determines the good or bad percolation capacity of the reservoir, which is directly related to the gas content of the reservoir, and provides help to clarify the gas content situation in the construction area of Funci Highway Tunnel.

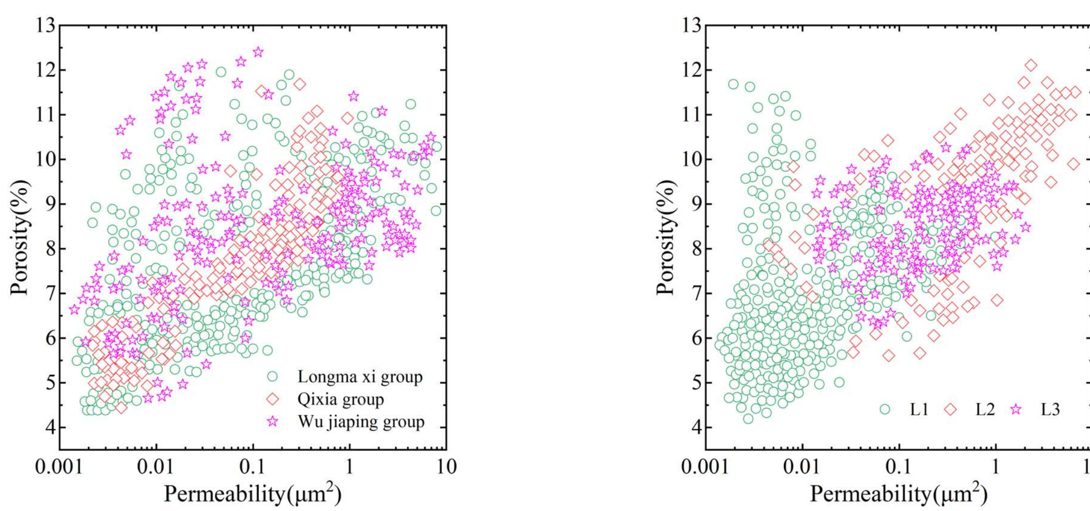

(a) Different areas (b) Different reservoir sandstone

Fig. 7. Fracture development results

4.1.3. Low-frequency characterization of gas-bearing reservoirs. Fenghongshan Tunnel passes through the strongly weathered tuff and moderately weathered tuff of Permian System, moderately weathered tuff of Fengning Group of Carboniferous System, moderately weathered shale sandstone of Upper Devonian System, Saibang Formation of Upper Silurian System, Luojaping Formation of Middle Silurian System, without crossing the hydrocarbon rock layer, and the tectonic movement is strong, and the strata are inverted. Taking the rock data of Fenghongshan Tunnel in the construction area of Furnace Ci Highway Tunnel as an example, the logging curves are normalized, and then the layer velocity-burial depth relationship is converted by using acoustic data. Figure 8 shows the layer velocity-buried depth relationship of the chemical tuff and sandstone.

As can be seen from the figure, with the increase of burial depth, the layer velocity increases gradually, and when the burial depth increases from 150 m to 550 m, the layer velocity can reach up to 3.18*103 m/s. Among them, the layer velocity of the dry sandstone is the largest, followed by the water-bearing sandstone, then the mudstone and oil-bearing sandstone, and the layer velocity of the gas-bearing sandstone is the lowest. The layer velocity of gas-bearing sandstone is greatly reduced, which inevitably leads to a significantly lower frequency, and it is also an effective method to predict the distribution of gas layers in the sand body in the construction area of Funci Highway Tunnel by utilizing low-frequency attributes.

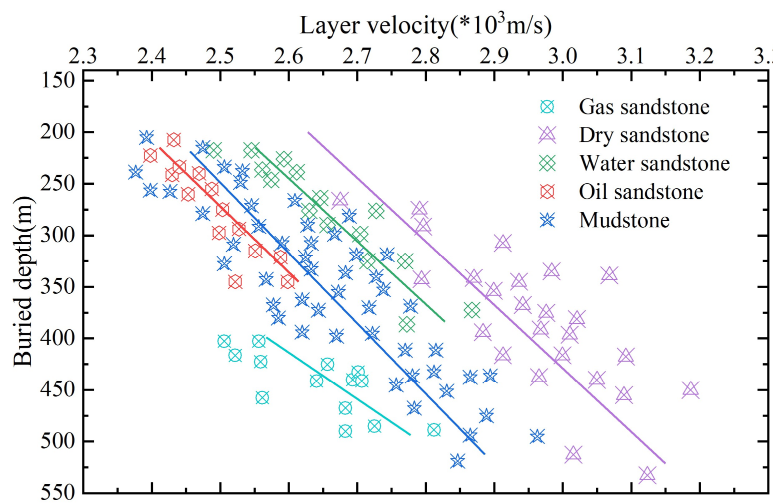

Fig. 8. Layer velocity - buried depth diagram

4.2. Analysis of pre-stack AVO inversion results

4.2.1. Wave impedance to velocity ratio. The pre-stack AVO inversion volume plate analysis is the key to differentiate shale gas layers from other shale gas-free enclaves and to distinguish how much shale gas layers contain. The known logging information (such as its transverse wave velocity, longitudinal wave velocity, density, etc.) in the test work area is utilized in combination with the reservoir information (such as Class I reservoir, Class II reservoir, Class III reservoir, non-reservoir, etc.) of its logs. Using the pre-stack AVO inversion model to analyze its intersection map and histogram, and using the longitudinal wave velocity, transverse wave velocity, density, and Poisson's ratio, longitudinal and transverse wave velocity ratio, Lamei's coefficient, etc., calculated from the three elasticity parameters, to differentiate between the enclosing rocks of the class I reservoir, class II reservoir, class III reservoir, and non-reservoir, which is conducive to the identification of the distribution of the shallow natural gas in the construction area of the Foucie Highway Tunnel.

Based on the pre-stack AVO inversion model and the inversion process given in the previous section, the Longmaxi Formation and the Qixia Formation in the Funci Highway tunnel construction area are selected for the wave impedance to wave velocity ratio solution. Figure 9 shows the intersection of wave impedance and wave velocity ratio of longitudinal and transverse waves in the region.

From the figure, it can be seen that the longitudinal wave velocity ratios of the non-reservoirs are mainly distributed between 1.59 and 1.86, while the longitudinal wave velocity ratios of the class I reservoirs are between 1.44 and 1.63, the longitudinal wave velocity ratios of the class II reservoirs are located between 1.45 and 1.69, and the longitudinal wave velocity ratios of the class III reservoirs have a wider distribution range of the longitudinal wave velocity ratios between 1.45-1.86. Longitudinal wave velocity ratios, which can be well differentiated from the class I reservoirs, class II reservoirs and non-reservoir surrounding rocks. However, the range of the longitudinal and transverse wave velocity ratios of the three types of reservoirs is too broad, which makes it difficult to distinguish the three types of reservoirs and non-reservoir surrounding rocks. Therefore, the longitudinal-transverse wave velocity ratios could not distinguish between shale-gas-free enclosing rocks and gas-bearing Class I storage, Class II reservoirs, and Class III reservoirs. Whereas the range of longitudinal wave impedance of class I storage is between 0.55-0.99, the distribution of longitudinal wave impedance of class II storage is between 0.63-1.33, the distribution of longitudinal wave impedance of class III storage is between 0.73-1.38, and the distribution of longitudinal wave impedance of non-reservoir enclosing rock is between 1.48-2.01, which shows that longitudinal wave impedance is able to distinguish perfectly between the gas-bearing It can be seen that the longitudinal wave impedance can perfectly distinguish the gas-containing Class I reservoirs, Class II reservoirs, Class III reservoirs, and gas-free non-reservoir surrounding rocks. Therefore, longitudinal wave impedance is the key parameter to distinguish gas-bearing reservoirs and non-reservoir surrounding rocks. During the construction of the tunnel of Funci Highway, the change of longitudinal and transverse wave impedance in each area can be clarified to determine whether the shallow natural gas is contained or not.

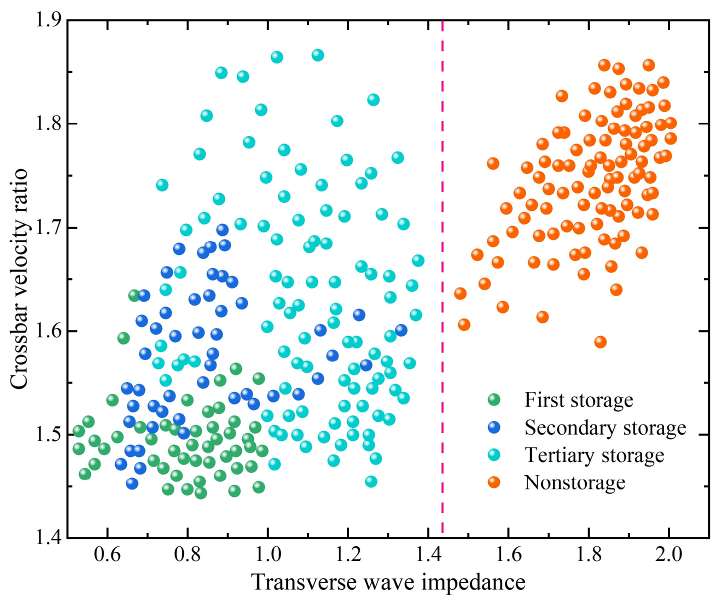

Fig. 9. Wave impedance and velocity ratio

4.2.2. Inversion results of different methods. Based on the analysis results in the previous section, multiple angular channel sets are obtained by stacking the pre-stacked channel sets by angles, and sub-waves are extracted from each angular channel set for inversion, and AVO inversion and the inversion method based on adaptive hybrid paradigm method (AHN) are used to compare the pre-stacked inversion. Figure 10 shows the results of the comparison between the inversion results of different methods and the original logging curves, in which Figure 10(a)~(b) shows the longitudinal wave velocity inversion results of the two methods, and Figure 10(c)~(d) shows the density inversion results of the two methods.

As can be seen from the figures, the longitudinal wave velocity and density obtained by using the pre-stack AVO inversion model have good correlation with the original logging curves from the general trend, and the error of the two is only 2.04% at the highest. On the other hand, the inversion method based on the adaptive mixed-paradigm approach has a large difference with the original log curve, and its error value can be up to 5.78%. This shows that the pre-stack AVO inversion model designed in this paper can effectively obtain the longitudinal wave velocity and density variations in the study area, better reflecting the gas content variations in different reservoirs, and the inversion results are in good agreement with the geological conditions. The inversion results can clearly reveal the interface between sandstone and shale, the lithology is clearly differentiated, the longitudinal wave velocity and density have obvious low value anomalies in the target layer section, and the high-velocity carbonate rock below the target layer shows high longitudinal wave velocity and high density characteristics, which is consistent with the results of the actual drilling. Relying on the pre-stack AVO inversion results, the shallow natural gas changes in the study area can be clarified, which will provide data support for the tunnel construction of Fuzi Expressway to avoid the risk area and enhance the construction safety.

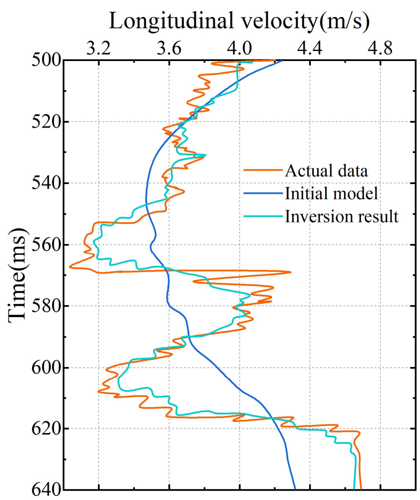

(a) AVO-Longitudinal velocity

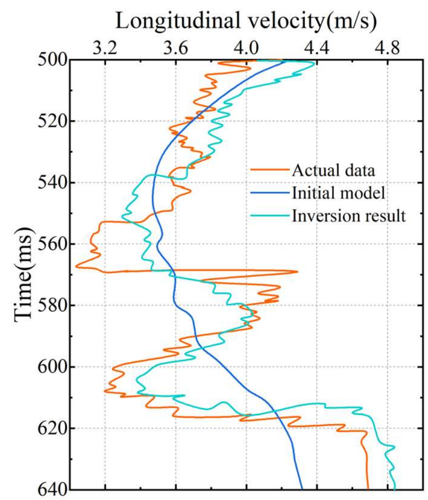

(b) AHN-Longitudinal velocity

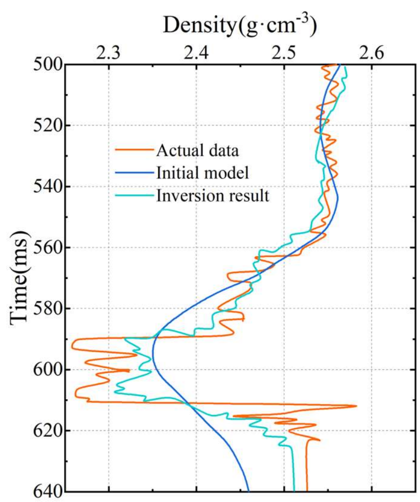

(c) AVO-Density

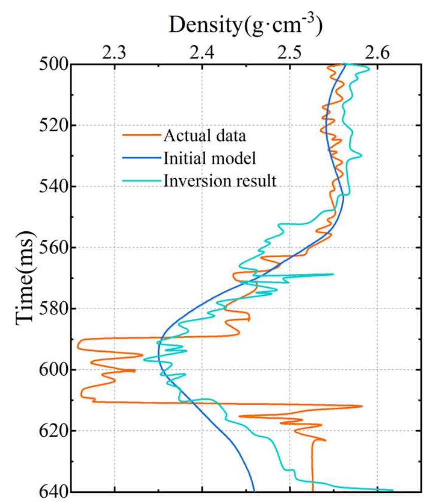

(d) AHN-Density

Fig. 10. Different methods of inversion results

4.3. Furnace Ci Expressway Tunnel Oil and Gas Evaluation

In this section, the Jianfengling Tunnel in Funci Block and the Chenjiapo Tunnel in Sangzhi Block are mainly selected to carry out oil and gas evaluations as a way to provide data support for the safety construction program of the Funci Expressway tunnel construction.

4.3.1. Furnace Ci Block - Tsim Sha Tsui Tunnel, Jianfengling Tunnel crosses the Quaternary System, Zhiliu System Saibao Formation and Luojiaoping Formation, and does not cross the hydrocarbon source layer, but the underlying Longmaxi Formation is an excellent hydrocarbon source rock, and it is not excluded that there is a small amount of shallow natural gas, and there is no natural gas showing in shallow natural gas testing of the Jianfengling Tunnel's 01 and 02 holes, which comprehensively evaluates that the Jianfengling Tunnel is a micro-gas tunnel. Based on the logging data given in the previous section, the sample test data of Jianfengling Tunnel in Fenzhi block are counted, and the oil and gas evaluation results of Jianfengling Tunnel boreholes are shown in Table 1.

Jianfengling Tunnel holes 01 and 02 were drilled to encounter the Saibang Formation, and the organic matter abundance of the drilled rock formation is non-hydrocarbon source rock, the maturity of organic matter is immature, oil-bearing zone, the organic matter type is type III, and the hydrocarbon potential is extremely poor. The evaluation of Jianfengling Tunnel holes 01 and 02 is no gas. Jianfengling Tunnel boreholes 01 and 02 mainly pass through shale and mudstone strata, except for the mudstone at 98.51~98.72m in Jianfengling Tunnel borehole 02, which is a very low porosity and low permeability reservoir with very poor reservoir performance, and the rest of them are low porosity and very low permeability reservoirs with average reservoir performance. The evaluation of Jianfengling Tunnel 01 hole is low gas, and Jianfengling Tunnel 02 hole is micro gas.

Overall, the two drill holes of Jianfengling Tunnel have very poor hydrocarbon potential and average reservoir performance, and Jianfengling Tunnel has not traversed the hydrocarbon rock layer. The two boreholes of Jianfengling Tunnel have no gas measurement, and the shallow natural gas test shows no natural gas, so the gas content is very poor. The comprehensive evaluation is a micro-gas tunnel. During tunnel construction, strengthen the prediction and monitoring of shallow natural gas, and strengthen tunnel ventilation.

Table 1. Sample test data statistics

Tunnel name	Jianfengling tunnel-01		Jianfengling tunnel-02	
Sampling depth	21.35~21.51	58.42~58.53	76.74~76.87	98.51~98.72
Lithology	Shale	Shale	Mudstone	Mudstone
Porosity	2.21%	3.03%	2.53%	0.67%
Permeability	0.003μm^2	0.011μm^2	0.011μm^2	0.002μm^2
TOC	0.158	0.076	0.069	0.085
Tmax	446.5	332.7	335.8	431.9
IH	48.06	29.14	45.49	38.63
D	4.73	3.65	4.92	3.98

4.3.2. Sangchu Block-Chenjiapo Tunnel. Chenjiapo Tunnel passes through the Quaternary, Permian Maokou Formation, Qixia Formation, and the middle Silurian Xiaoxiyu Formation, and crosses the hydrocarbon source rock layer of the Qixia Formation. Although the Qixia Formation passes through the sky, and the downward mobility of the layer is strong, the inclination angle of the rock layer is small, and the faults are occasionally seen in between the layers, and the fracture and cleavage are more developed. Table 2 shows the statistics of the sample test data of Chenjiapo Tunnel.

1) Geochemical characteristics. Chenjiapo Tunnel hole 05 drilled Maokou Formation, 145.38m,

153.47m drilled rock layer organic matter abundance is excellent hydrocarbon source rock, organic matter maturity is oil-bearing zone, organic matter type is Ⅲ, the potential for hydrocarbon is general, evaluation of Chenjiapo Tunnel hole 05 for low gas.

2) Reservoir characteristics. Chenjiapo Tunnel borehole 05 mainly passes through tuff, carbonaceous mudstone and dolomite strata, special low porosity and low permeability reservoir, with very poor reservoir performance, evaluating Chenjiapo Tunnel borehole 05 as no gas.

Overall, the hydrocarbon potential of Chenjiapo Tunnel borehole 05 is average, with very poor reservoir performance, and Chenjiapo Tunnel passes through the hydrocarbon source rock layer of Qixia Formation. There is no obvious gas anomaly in one borehole of Chenjiapo Tunnel, no natural gas in shallow natural gas test, and the absolute gas outflow is 0, which is poor in gas content. It is evaluated as a low-gas tunnel. During tunnel construction, strengthen the prediction and monitoring of shallow natural gas, and enhance tunnel ventilation.

Table 2. Sample test data statistics

Tunnel name	Chenjiapo tunnel -05			
Sampling depth	91.54~91.72	145.38~145.72	153.47~153.81	176.42~176.94
Lithology	Limestone	Carbonite	Carbonite	Dolomite
Porosity	1.48%	/	/	1.31%
Permeability	0.002μm^2	/	/	0.006μm^2
TOC	0.735	5.742	5.679	0.498
Tmax	476.7	442.9	461.8	379.5
IH	2.115	5.478	4.182	2.051
D	0.276	0.563	0.406	0.294

5. Conclusion

This paper takes the high speed tunnel construction area from Fenghongshan to Cili County as an example, and constructs a natural gas inversion model by using AVO technology to carry out data analysis and comprehensive evaluation of the regional reservoir characteristics and shallow natural gas in the Fenghongshan-Cili high speed tunnel construction. The porosity of the rock layer in the tunnel construction area of Funci Highway ranges from 4.5% to 12%, with an average porosity of 8.93% and a maximum permeability of 0.004 μm^2. When the burial depth increases from 150 m to 550 m, the maximum layer velocity can reach 3.18*103 m/s. In the results of pre-stack AVO inversion, the distribution of longitudinal wave impedance of the non-reservoir surrounding rock ranges from 1.48-2.01, and the error between the longitudinal wave velocity and density obtained from the inversion and the original logging curves is only 2.04% at the highest. Based on the logging data, we can effectively realize the shallow natural gas distribution in Funci Highway Tunnel, and analyze the oil and gas distribution in different areas by combining the statistical data, so as to provide data support for improving the construction safety and risk avoidance ability of Funci Highway Tunnel.

References

[1] Chapman, D. N., Metje, N., & Stark, A. (2017). Introduction to tunnel construction. Crc Press.

[2] Song, Z., Shi, G., Wang, J., Wei, H., Wang, T., & Zhou, G. (2019). Research on management and application of tunnel engineering based on BIM technology. Journal of Civil Engineering and Management, 25(8), 785-797.

[3] Wang, X., Lu, H., Wei, X., Wei, G., Behbahani, S. S., & Iseley, T. (2020). Application of artificial neural network in tunnel engineering: a systematic review. IEEE Access, 8, 119527-119543.

[4] Vvedenskij, R. V., Gendler, S. G., & Titova, T. S. (2018). Environmental impact of the tunnel construction. Magazine of Civil Engineering, (3 (79)), 141-150.

[5] Moretti, L., Cantisani, G., & Di Mascio, P. (2016). Management of road tunnels: Construction, maintenance and lighting costs. Tunnelling and Underground Space Technology, 51, 84-89.

[6] Ye, F., Han, X., Qin, N., Ouyang, A., Liang, X., & Xu, C. (2020). Damage management and safety evaluation for operating highway tunnels: a case study of Liupanshan tunnel. Structure and Infrastructure Engineering, 16(11), 1512-1523.

[7] Xu, J., Guo, C., & Yu, L. (2019). Factors influencing and methods of predicting greenhouse gas emissions from highway tunnel construction in southwestern China. Journal of Cleaner Production, 229, 337-349.

[8] Wu, B., & Sun, W. (2024). A Method for Calculating the Instability Probability in a Deeply Buried Tunnel Construction with a Hidden Karst Cave at the Bottom. Applied Sciences, 14(5), 1691.

[9] Wang, J., Cao, A., Wu, Z., Sun, Z., Lin, X., Sun, L., ... & Long, Y. (2021). Dynamic risk assessment of ultra-shallow-buried and large-span double-arch tunnel construction. Applied Sciences, 11(24), 11721.

[10] Diao, S., Shi, B., & Liu, X. (2024). Research on two-dimensional imaging method of tunnel water hazard hidden danger based on magnetic resonance rotation detection. AIP Advances, 14(1).

[11] Huang, X., Li, S., Xu, Z., Guo, M., & Chen, Y. (2018). Assessment of a concealed karst cave's influence on karst tunnel stability: a case study of the huaguoshan tunnel, China. Sustainability, 10(7), 2132.

[12] Yang, R., & Deng, Y. (2021, February). Analysis on security risks in tunnel construction based on the fault tree analysis. In IOP Conference Series: Earth and Environmental Science (Vol. 638, No. 1, p. 012089). IOP Publishing.

[13] Qian, J., & Zhou, Y. (2021, July). Study on quality and safety monitoring scheme of tunnel construction based on 3D laser scanning. In IOP Conference Series: Earth and Environmental Science (Vol. 804, No. 2, p. 022073). IOP Publishing.

[14] Yang, J., Wu, S., Tong, G., Wang, H., Guo, Y., Zhang, W., ... & Xu, F. (2022). Acoustic prediction and risk evaluation of shallow gas in deep-water areas. Journal of Ocean University of China, 21(5), 1147-1153.

[15] Cox, D. R., Huuse, M., Newton, A. M., Sarkar, A. D., & Knutz, P. C. (2021). Shallow gas and gas hydrate occurrences on the northwest Greenland shelf margin. Marine Geology, 432, 106382.

[16] Müller, S., Reinhardt, L., Franke, D., Gaedicke, C., & Winsemann, J. (2018). Shallow gas accumulations in the German North Sea. Marine and Petroleum Geology, 91, 139-151.

[17] Shi, K., Feng, Y., Gao, P., Fan, Q., Li, Q., Leng, S., ... & Song, Y. (2024). Enhancing gas hydrate decomposition assisted by the shallow gas: Effects of interlayer permeability and depressurization strategies. Fuel, 374, 132477.

[18] Guan, Z., Wang, Y., Cao, Z., & Hong, Y. (2020). Smart sampling strategy for investigating spatial distribution of subsurface shallow gas pressure in Hangzhou Bay area of China. Engineering geology, 274, 105711.

[19] Chen, Y., Deng, B., & Zhang, J. (2020). Shallow gas in the Holocene mud wedge along the inner East China Sea shelf. Marine and Petroleum Geology, 114, 104233.

[20] Xudong Zhang,Cheng Yin & Gulan Zhang. (2021). Confirmation of AVO Attribute Inversion Methods for Gas Hydrate Characteristics Using Drilling Results from the Shenhu Area, South China Sea. Pure and Applied Geophysics(2),1-14.

[21] K.P. Arun,Kalachand Sain & Jitender Kumar. (2020). Application of constrained AVO inversion: 2-D modelling of gas hydrates and free gas in Mahanadi basin, India. Journal of Natural Gas Science and Engineering(prepublish).

[22] Xiangchun Wang,Dongyang Pan,Zhongliang Wu & Qingxian Zhao. (2018). Gas hydrate elastic properties inversion by AVO Technology in Shenhu Area of the South China Sea. Arabian Journal of Geosciences(18),1-9.